THE JOURNAL OF BIOLOGICAL CHEMISTRY VOL. 282, NO. 18, pp. 13813–13823, May 4, 2007

Auto-inhibition of the Dbl Family Protein Tim by an N-terminal Helical Motif*

Received for publication, January 8, 2007, and in revised form, March 1, 2007 Published, JBC Papers in Press, March 2, 2007, DOI 10.1074/jbc.M700185200

Marielle E. Yohe[‡], Kent L. Rossman[‡§1], Olivia S. Gardner[¶2], Antoine E. Karnoub[§2], Jason T. Snyder[‡], Svetlana Gershburg[‡], Lee M. Graves[‡], Channing J. Der[‡§3], and John Sondek[‡§‖4]

From the Departments of [‡]Pharmacology and [‖]Biochemistry and Biophysics, [§]Lineberger Comprehensive Cancer Center, [¶]Curriculum in Toxicology, University of North Carolina, Chapel Hill, North Carolina 27599-7295

Dbl-related oncoproteins are guanine nucleotide exchange factors specific for Rho-family GTPases and typically possess tandem Dbl homology (DH) and pleckstrin homology domains that act in concert to catalyze exchange. Because the ability of many Dbl-family proteins to catalyze exchange is constitutively activated by truncations N-terminal to their DH domains, it has been proposed that the activity of Dbl-family proteins is regulated by auto-inhibition. However, the exact mechanisms of regulation of Dbl-family proteins remain poorly understood. Here we show that the Dbl-family protein, Tim, is auto-inhibited by a short, helical motif immediately N-terminal to its DH domain, which directly occludes the catalytic surface of the DH domain to prevent GTPase activation. Similar to the distantly related Vav isozymes, auto-inhibition of Tim is relieved by truncation, mutation, or phosphorylation of the auto-inhibitory helix. A peptide comprising the helical motif inhibits the exchange activity of Tim *in vitro*. Furthermore, substitutions within the most highly conserved surface of the DH domain designed to disrupt interactions with the auto-inhibitory helix also activate the exchange process.

RhoA, Rac1, and Cdc42 are the best understood of the 22 human Rho-family GTPases, which comprise one of five branches of the Ras superfamily of small GTPases (1). Like Ras, Rho proteins function as binary switches that alternate between inactive, GDP-bound states and active, GTP-bound states. Once activated, Rho GTPases directly engage numerous downstream effectors to modulate their functions. Active Rho GTPases and their effectors orchestrate actin cytoskeleton rearrangement and gene transcription to coordinate diverse cellular processes including adhesion, migration, phagocytosis, cytokinesis, neurite extension and retraction, polarization, growth, and survival (2). Not surprisingly, aberrant activation of Rho GTPases promotes various developmental, immunological, and proliferative disorders (3).

The Dbl-family of guanine nucleotide exchange factors (GEFs)[5] are the largest group of proteins directly responsible for the activation of Rho GTPases. Dbl-family proteins are characterized by a Dbl-homology (DH) domain, which contacts the Rho GTPase to catalyze nucleotide exchange, and an associated pleckstrin homology (PH) domain, which fine-tunes the exchange process by a variety of mechanisms related to the binding of phosphoinositides. The 69 human Dbl-family proteins are divergent in regions outside the DH/PH module, and contain additional domains that presumably dictate unique cellular functions (4).

The capacity of DH domains to activate Rho GTPases is tightly regulated through a multitude of diverse mechanisms ranging from alterations in transcript levels and protein expression (5) to subcellular re-distribution (6), post-translation modifications (7), and protein degradation (8). However, despite this large spectrum of regulatory mechanisms, in most cases, truncation of Dbl-family proteins often potently activates their exchange activities (9). Currently, there is no general understanding for why truncation promotes unregulated exchange.

To better understand potential mechanisms that regulate Dbl-family proteins, we have chosen to study the relatively small, human Dbl-member, Tim (transforming immortalized mammary). Tim was originally identified based upon its capacity to induce transformation of NIH 3T3 cells upon truncation (10), and whereas there are multiple transcripts of TIM (10, 11), endogenous Tim is expressed as a 60-kDa protein, consisting of a short N-terminal region (~70 residues) followed by a DH/PH cassette and an adjacent C-terminal SH3 domain. All conserved homologs of Tim preserve this domain architecture. mRNA transcripts encoding Tim are expressed in numerous tissues and cancer-derived cell lines; corresponding protein expression has been verified in various cell lines (10, 11). The gene encoding human Tim has been localized to chromosomal region 7q33–7q35, which has been implicated in rearrangements contributing to both acute myelogenous leukemia and breast carcinoma (12). Nonetheless, whereas Tim was originally identified as an oncogene, its *in vivo* functions and regulation are unknown. Indeed, although Tim was cloned from a cDNA expression library derived from a human mammary epithelial cell line, Tim expression is down-regulated in breast carcinoma

* The costs of publication of this article were defrayed in part by the payment of page charges. This article must therefore be hereby marked "*advertisement*" in accordance with 18 U.S.C. Section 1734 solely to indicate this fact.
[1] Supported by the American Cancer Society.
[2] Supported by the Susan G. Komen Breast Cancer Foundation.
[3] Supported by National Institutes of Health Grants CA92240 and CA063071.
[4] Supported by National Institutes of Health Grants GM65533 and GM62299. To whom correspondence should be addressed: CB #7365, 1106 M. E. J. Bldg., Chapel Hill, NC 27599. Tel.: 919-966-7350; E-mail: Sondek@med.unc.edu.

[5] The abbreviations used are: GEF, guanine nucleotide exchange factor; Tim, transforming immortalized mammary; DH, Dbl homology; PH, pleckstrin homology; SH3, Src homology 3; GST, glutathione *S*-transferase; mant-GTP, methylanthraniloyl-GTP; HEK, human embryonic kidney; HA, hemagglutinin.

cell lines and aggressive primary breast carcinoma cells express versions of Tim in which the catalytic DH domain is either truncated or mutated, suggesting a possible tumor suppressor function for Tim (13).

Here we show that the exchange potential of Tim toward RhoA is inhibited by a short N-terminal region with high helical propensity that directly interacts with the DH domain to prevent access of Rho GTPases to the DH domain. Truncation, mutation, or phosphorylation of this putative helix fully relieves this auto-inhibition. Addition of the putative helix in *trans* to truncated Tim restores inhibition. Furthermore, a substitution within the DH domain designed to disrupt interactions with the N-terminal helix also relieves auto-inhibition. These results show that Tim, like the distantly related Vav isozymes, is activated by unintentional truncation and regulated phosphorylation.

EXPERIMENTAL PROCEDURES

Protein Expression and Purification—Full-length and truncated versions of human Tim were PCR-amplified and ligated into pET-21a (Novagen) between NdeI and XhoI. The cDNA for Tim was a gift of Dr. David Siderovski (University of North Carolina).

Tim constructs were expressed in the *Escherichia coli* strain Rosetta (DE3) (Novagen). Cell cultures were grown at 37 °C in LB/ampicillin (100 μg/ml), and induced with 1 mM isopropyl β-D-thiogalactopyranoside for 5 h at 27 °C. Cell pellets were resuspended in 20 mM HEPES, pH 7, 1 mM EDTA, 2 mM dithiothreitol, 10% glycerol (buffer A) containing 20 mM NaCl, lysed using an Emulsiflex C5 cell homogenizer (Avestin), and clarified by centrifugation at 40,000 × *g* for 45 min at 4 °C. Clarified supernatant was loaded on a Fast Flow S column (GE Healthcare) equilibrated with buffer A and eluted with a linear gradient of 20–500 mM NaCl. Tim protein eluted at ~300 mM NaCl and was loaded onto an S-200 size exclusion column (GE Healthcare) equilibrated with buffer A containing 300 mM NaCl. Fractions containing monomeric Tim were pooled, concentrated, and stored at −80 °C. Mutations were introduced into wild-type Tim using the QuikChange site-directed mutagenesis kit (Stratagene) as per the manufacturer's instructions, and these mutant proteins were expressed and purified as described above. DNA sequences of all expression constructs were verified by automated sequencing. RhoA was purified as described (14–16).

Baculoviruses encoding both the wild-type and kinase inactive (K297A) versions of the kinase domain of c-Src (*Mus musculus*) were generated from pFastBacHT vectors (gifts of Dr. David Siderovski, UNC) using the Bac-to-Bac method (Invitrogen). HighFive insect cells were infected with the baculovirus at a multiplicity of infection of 1.0. After 48 h of incubation at 27 °C, cells were harvested by low speed centrifugation, resuspended, and lysed in 20 mM HEPES, pH 7.5, 500 mM NaCl, 2 mM $MgCl_2$, 10% glycerol (buffer B) with 10 mM imidazole, and clarified by centrifugation at 100,000 × *g* for 45 min. The clarified supernatants were diluted to a final volume of 150 ml and loaded onto a nickel-charged metal chelating column (GE Healthcare) equilibrated with buffer B containing 10 mM imidazole, washed with buffer B containing 50 mM imidazole and eluted with buffer B containing 400 mM imidazole. Eluted Src was extensively dialyzed *versus* buffer B with 150 mM NaCl and 1 mM EGTA, concentrated, and stored at −80 °C.

The kinase domain of EphA4 was PCR amplified from the full-length cDNA (gift of N. Mochizuki, National Cardiovascular Center Research Institute, Suita, Osaka, Japan), ligated into pGEX4T2 (Amersham Biosciences) in frame with an N-terminal GST tag, and expressed in BL21(DE3) *E. coli* as described above. Cell pellets were resuspended in 20 mM Tris, pH 7.5, 150 mM NaCl, 1 mM EDTA, 2 mM dithiothreitol, 10% glycerol (buffer C), lysed, and clarified as described above. Clarified lysate was loaded onto a glutathione-Sepharose column (GE Healthcare). EphA4 protein was washed and eluted in buffer C containing 10 mM glutathione. The GST tag was removed with TEV protease and protein was loaded on an S-200 column equilibrated with buffer C. Eluted EphA4 was concentrated and stored at −80 °C.

Guanine Nucleotide Exchange Assays—Fluorescence spectroscopic analysis of *N*-methylanthraniloyl (mant)-GTP incorporation into RhoA was carried out as described (17). In brief, assay mixtures containing 20 mM Tris, pH 7.5, 150 mM NaCl, 5 mM $MgCl_2$, 1 mM dithiothreitol, and 100 μM mant-GTP (Molecular Probes) and 2 μM RhoA were allowed to equilibrate with continuous stirring. After equilibration, 50 nM Tim was added and nucleotide loading was monitored as the decrease in the tryptophan fluorescence (λ_{ex} = 295 nm, λ_{em} = 335 nm) of RhoA or the increase in the mant-GTP fluorescence (λ_{ex} = 360 nm, λ_{em} = 440 nm) as a function of time using a PerkinElmer Life Sciences LS 55 spectrophotometer. Rates of guanine nucleotide exchange were determined by fitting the data to a single exponential decay model with GraphPad Prizm. Data were normalized to yield percent GDP released and assays were performed in duplicate.

Cell Culture and Transformation Assays—NIH 3T3 mouse fibroblasts were maintained in Dulbecco's modified Eagle's medium supplemented with penicillin/streptomycin and 10% calf serum (Hyclone). HEK 293T cells and SYF fibroblasts were maintained in Dulbecco's modified Eagle's medium supplemented with penicillin/streptomycin and 10% fetal bovine serum (Sigma). PCR-amplified Tim constructs were ligated into pcDNA 3.1 Hygro (Invitrogen) between EcoRI and XhoI such that an expressed HA-tag was encoded at the N terminus of each construct. Mutations were introduced into wild-type Tim as described above.

Cell lines stably expressing Tim were established by transfecting NIH 3T3 cells with 1 μg of each pcDNA construct using Lipofectamine Plus (Invitrogen) according to the manufacturer's protocol. Three days post-transfection the cells were subcultured into growth medium supplemented with 300 μg/ml of hygromycin B. Mass populations of multiple, drug-resistant colonies (>50) were pooled together for focus formation analyses. Western blot analysis with an anti-HA antibody (Covance) was performed to verify Tim expression in the cell lines.

For the secondary focus formation assays, equal numbers of cells from each cell line were seeded into 60-mm dishes. The growth medium of each dish was replaced with fresh hygromycin-supplemented medium every 3 days. 14 days after seeding, the dishes were stained with crystal violet and the foci were

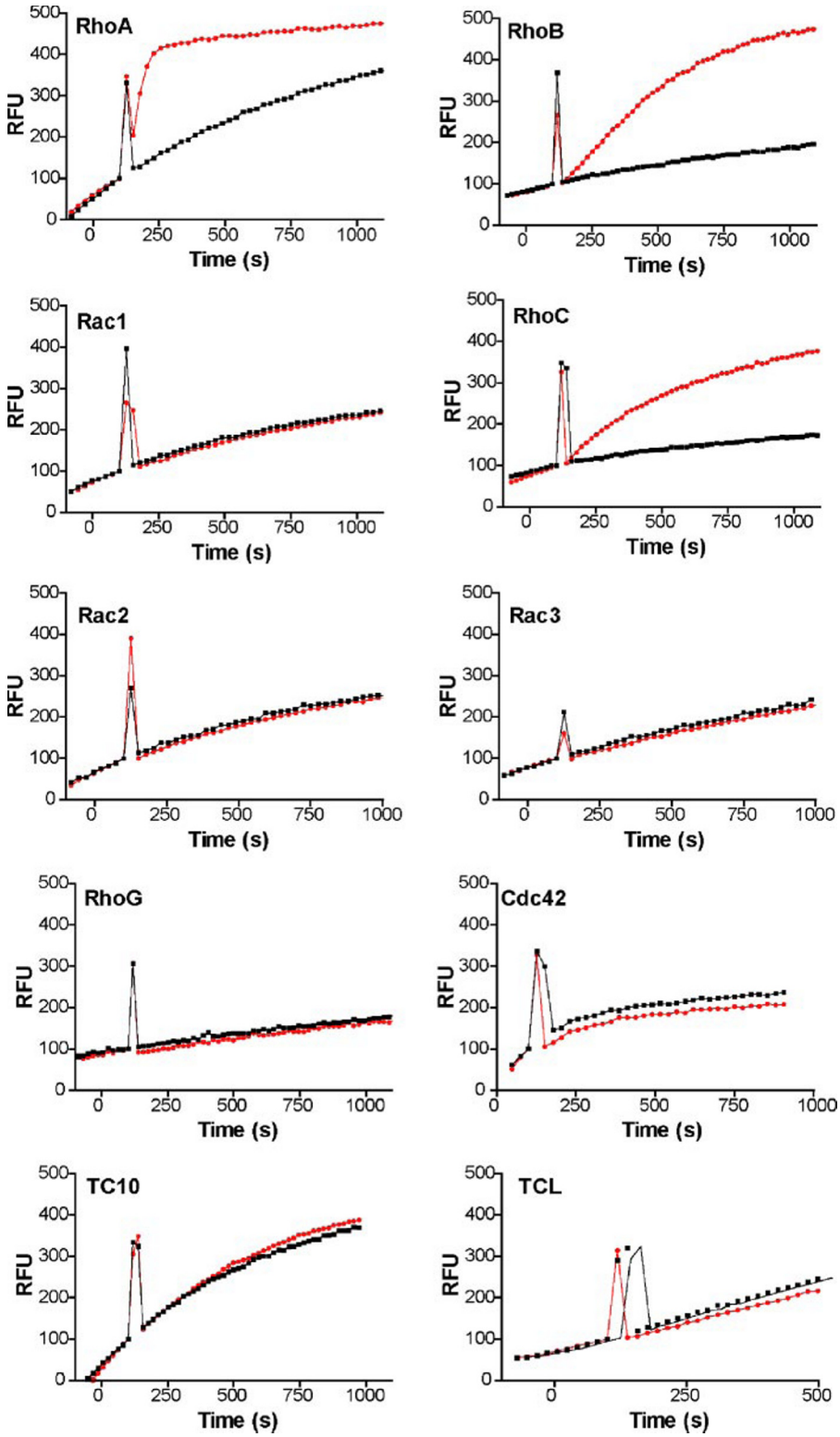

FIGURE 1. **Tim is specific for RhoA, RhoB, and RhoC.** The exchange of GDP bound to various Rho GTPases and catalyzed by Tim was measured using a standard fluorescence-based assay (14, 17). The relative fluorescence units (*RFU*) resulting from mant-GTP loading onto each GTPase are shown for Tim catalyzed (*red curves*) and intrinsic (*black curves*) exchange reactions. The GTPases were purified and assessed for GTP loading stimulated by EDTA as previously described (51).

quantified by visual inspection. Individual experiments were performed in duplicate and independently carried out three times.

GTPase Activation Assays—Affinity purifications of RhoA were carried out as described (18). In brief, the Rho binding domain of Rhotekin (amino acids 7–89) was expressed as a GST fusion protein in BL21(DE3) cells and immobilized on glutathione-coupled Sepharose 4B beads (Amersham Biosciences). HEK 293T cells were transiently transfected with 1 μg of various pcDNA-Tim constructs using Lipofectamine 2000 (Invitrogen) according to the manufacturer's protocol. Immediately post-transfection, these cells were serum starved in Dulbecco's modified Eagle's medium supplemented with 0.1% fetal bovine serum and incubated for 16 h. Cells were washed in ice-cold phosphate-buffered serum and lysed in lysis buffer (50 mM Tris, pH 7.5, 500 mM NaCl, 30 mM $MgCl_2$, 0.1% SDS, 0.5% sodium deoxycholate, 1.0% Triton X-100 and protease inhibitors). Lysates were clarified by centrifugation at 16,000 $\times$ *g* for 10 min. Total protein concentration of the lysates was determined by a colorimetric assay (Bio-Rad). 1 mg of clarified HEK 293T lysate was incubated with 120 μg of GST-Rhotekin-Rho binding domain beads for 1 h at 4 °C. The beads were washed three times in wash buffer (25 mM Tris, pH 7.5, 30 mM $MgCl_2$, 40 mM NaCl and protease inhibitors). Total and affinity purified lysates were subjected to SDS-PAGE and Western blot analysis using an anti-RhoA (Santa Cruz Biotechnology) monoclonal antibody. Each experiment was performed a minimum of three times. Precipitation of Tim with recombinant G17A RhoA was performed essentially as described (19).

In Vitro Kinase Assay—30 μg of purified Tim protein was incubated with 250 ng of recombinant Src or EphA4 kinase domain in kinase buffer (100 mM Tris, pH 7.5, 125 mM $MgCl_2$) supplemented with 100 μM ATP and 5 μCi of [γ-^{32}P]ATP for 60 min at 30 °C. Samples were subjected to SDS-PAGE and autoradiography. Control substrate peptide was obtained from Upstate.

Immunoprecipitation—The cDNAs for various Src constructs in pUSEamp were obtained from Upstate. SYF fibro-

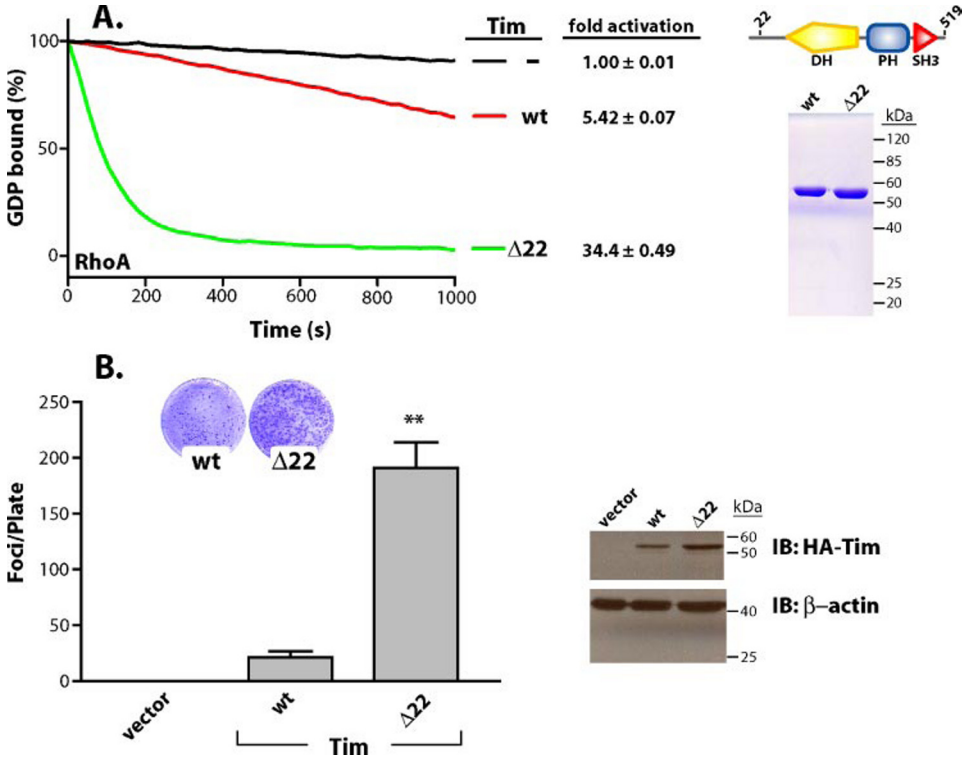

FIGURE 2. **Full-length Tim is auto-inhibited by its N-terminal region.** *A*, the exchange of GDP bound to RhoA and catalyzed by Tim was measured using a standard fluorescence-based assay (14, 17). -Fold activation is relative to the spontaneous loading of guanine nucleotide and represents the average of two independent reactions for each trace. Equal amounts (2 μg) of purified proteins used in the exchange assays are shown at the *right* following SDS-PAGE and staining with Coomassie Brilliant Blue. Also shown is a schematic of the domain architecture of Tim with the site of N-terminal truncation indicated. *B*, N-terminal truncated Tim potentiates transformation of NIH 3T3 cells. Data represent the averages of three independent experiments carried out in duplicate. ** denotes $p < 0.01$, as determined by a pairwise *t* test assuming equal variances. *Inset* illustrates representative plates of foci. *Right panel* verifies approximately equal expression of Tim variants used in the focus formation assays. *wt*, wild type; *IB*, immunoblot.

blasts were transfected with 10 μg of Src and 5 μg of Tim using Superfect (Qiagen) according to the manufacturer's protocol. 24 h post-transfection, the cells were serum starved in Dulbecco's modified Eagle's medium supplemented with 0.1% fetal bovine serum and incubated for 16 h. Cells were washed in ice-cold phosphate-buffered serum and lysed in lysis buffer. Lysates were clarified by centrifugation at 16,000 $\times$ *g* for 10 min. 1 mg of clarified SYF lysate was incubated with 25 μg of anti-HA affinity matrix (Roche) for 1 h at 4 °C. The beads were washed three times in lysis buffer. Total and affinity purified lysates were subjected to SDS-PAGE and Western blot analysis using anti-phosphotyrosine (Transduction Laboratories), anti-Src (Upstate), anti-HA (Covance), and anti-β-actin (Sigma) antibodies. The experiment was performed three times.

RESULTS

Specificity of the Guanine Nucleotide Exchange Activity of Tim—Previous studies by our laboratory have shown that Tim catalyzes exchange of guanine nucleotides on RhoA, but not on Rac1 or Cdc42 (16). This specificity of exchange activity is due to the fact that Tim possesses a basic residue in helix α5 of the DH domain, which is able to form an energetically favorable salt-bridge interaction with glutamate 54 of RhoA. Rac1 and Cdc42 does not have an acidic residue in the position analogous to Glu-54 of RhoA, and thus cannot make this contact with Tim (16). However, recent work in which Tim is overexpressed in various mammalian cell types suggests that Tim may catalyze exchange on more than one Rho family GTPase. For example, expression of Tim in COS-7 or NIH 3T3 cells leads to a loss of actin stress fibers and the formation of membrane ruffles, dorsal ruffles, and filopodia, suggesting that Tim may activate Rac1, RhoG, or Cdc42 but not RhoA in these cell types (13). However, expression of Tim in COS-7 cells leads to activation of RhoA, and not Rac1 or Cdc42, in pulldown experiments using GST-tagged versions of the Rho-binding domains of the Rho effector, Rhotekin, and the Rac1 and Cdc42 effector, Pak (11). In the same study, Tim expression in NIH 3T3 cells led to activation of JNK, SRF, and AP-1-regulated transcription, suggesting that Tim activates multiple GTPases in this cell type. However, in the same work, Tim expression in Swiss 3T3 cells led to cell rounding, whereas Tim expression in HeLa cells led to an increase in vinculin-enriched focal adhesions, suggesting that Tim activates RhoA in these cell types.

In an attempt to resolve these conflicting data, and to test the hypothesis that Tim activates multiple GTPases, we performed a fluorescence-based guanine nucleotide exchange assay on a library of Rho-family GTPases (Fig. 1). In this assay, Tim robustly activated each of the members of the RhoA subfamily of Rho GTPases, RhoA, RhoB, and RhoC. However, Tim failed to activate members of the Rac1 (Rac1, Rac2, Rac3, and RhoG) or Cdc42 (Cdc42, TCL, and TC10) subfamilies. These data suggest that Tim directly activates members of the RhoA subfamily of GTPases, but may indirectly activate additional GTPases when overexpressed in various cell types.

Regulation of Tim by Regions Preceding Its DH Domain—Tim was originally identified by its capacity to transform NIH 3T3 cells upon N-terminal truncation (10). Because many Dbl-family proteins are activated by similar truncations, we undertook a detailed analysis of the structural determinants within the N-terminal region of Tim required for its auto-inhibition. Using purified proteins, full-length Tim (*wt*, Fig. 2*A*) enhanced the rate of exchange of guanine nucleotide bound to RhoA by a modest 5-fold relative to the equivalent, spontaneous reaction (−). In contrast, truncation of the first 22 residues of Tim (Δ22) greatly enhanced the normalized loading of nucleotide by more than 30-fold.

Constitutive RhoA activation promotes cellular transformation, and consistent with the *in vitro* exchange data, stable

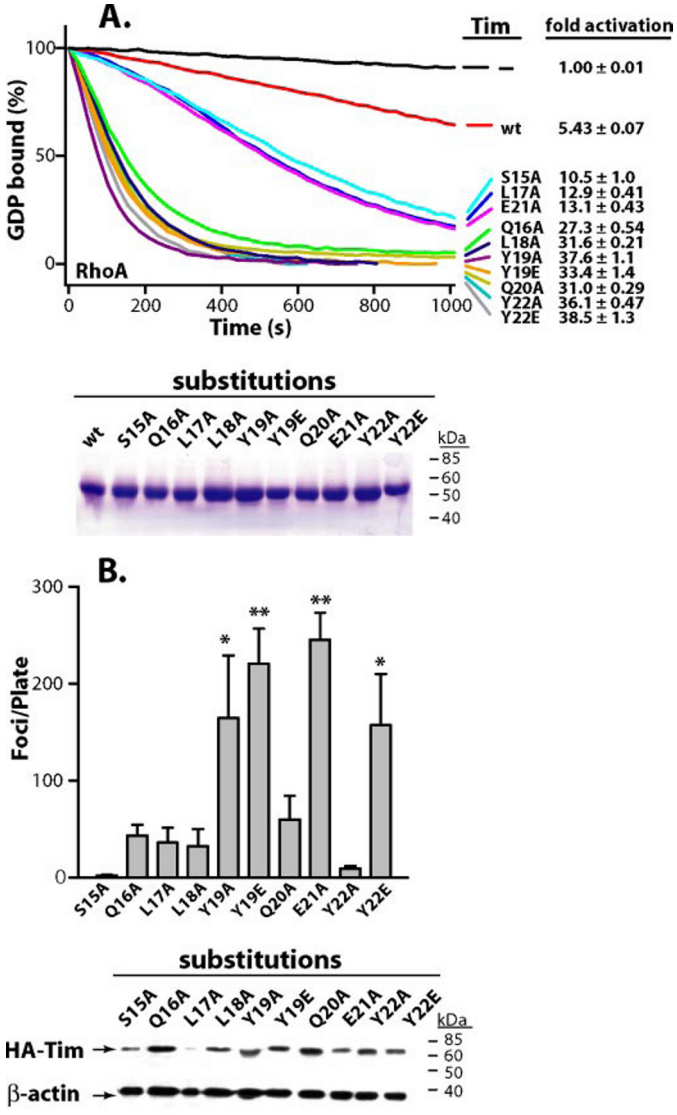

FIGURE 3. **A short region within Tim is responsible for auto-inhibition.** *A*, the N-terminal portion of Tim was subjected to scanning mutagenesis and the purified proteins were assayed for their capacity to catalyze the exchange of guanine nucleotides on RhoA. -Fold activation is relative to the spontaneous loading of nucleotide onto RhoA (−) and represents the average of two independent assays for each mutant. Equal amounts (2 μg) of purified proteins used in the exchange assays are shown in the *lower panel* following SDS-PAGE and staining with Coomassie Brilliant Blue (a composite of several gels is shown). *B*, equivalent forms of Tim were stably expressed in NIH 3T3 cells (*lower panel*, composite Western blot) and assayed for foci formation (*upper panel*). Data represent the averages of three independent experiments carried out in duplicate. *, denotes $p < 0.05$; **, denotes $p < 0.01$, as determined by a pairwise *t* test assuming equal variances. *wt*, wild type.

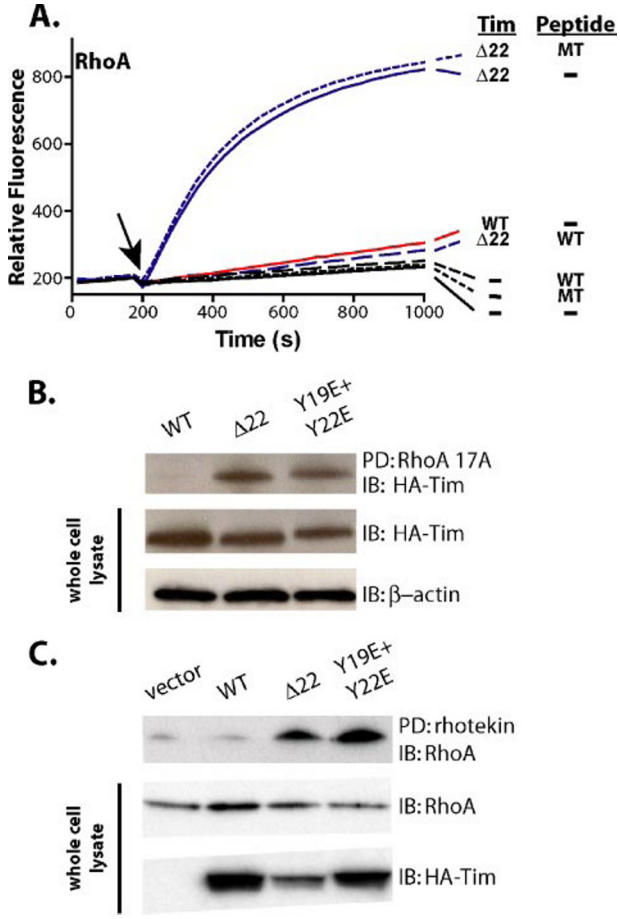

FIGURE 4. **The N-terminal region is necessary and sufficient for Tim auto-inhibition.** *A*, Tim (Δ22) was incubated with either a peptide corresponding to the N-terminal auto-inhibitory region (*WT*, biotin-SQLLYQEYSDV-amide) or a mutant peptide (*MT*, biotin-SQLLEQEYSDV-amide) at room temperature for 20 min. The resulting complexes were assayed for their ability to stimulate loading of mant-GTP onto RhoA. The peptide concentrations were 100 μM. *B*, the activity of Tim constructs transiently expressed in quiescent HEK 293T cells was assessed by a pulldown assay using GST-tagged nucleotide-free RhoA as the affinity purification matrix. Levels of active Tim were determined by immunoblotting the pulldown samples. Immunoblots (*IB*) of the total cell lysate (2.5% input shown) show approximately equal expression of the Tim constructs. *C*, the ability of Tim constructs to stimulate GTP loading on RhoA in HEK 293T cells was assessed by affinity precipitation of active RhoA with rhotekin. Levels of RhoA-GTP were determined by immunoblotting the affinity precipitated samples and were compared with RhoA pools in the total cell lysate (1% input shown). In the same experiment, HA-tagged Tim variants were checked for approximately equal expression by immunoblotting.

expression in NIH 3T3 cells of Tim (Δ22) promoted robust formation of foci relative to background (vector) and full-length Tim (wt) (Fig. 2*B*). The combined results from the *in vitro* exchange assays and cellular transformation assays indicate that Tim is auto-inhibited by its N terminus and that deletion of the first 22 residues of Tim relieves this auto-inhibition to promote robust guanine nucleotide exchange on RhoA *in vitro* as well as significant transformation of NIH 3T3 cells.

To produce a high-resolution map of the residues within the N-terminal portion of Tim necessary for auto-inhibition, this region was subjected to alanine-scanning mutagenesis and the resulting purified mutant proteins were tested for their capacity to activate RhoA *in vitro* (Fig. 3*A*). This analysis identified residues 15–22 of Tim as necessary for its auto-inhibition *in vitro*. Stable expression of these substituted forms of Tim in NIH 3T3 cells indicated an approximate direct correlation between the capacity of Tim to activate RhoA *in vitro* and the transformation potential of the mutated forms of Tim (Fig. 3*B*). One exception to this rule, Y22A, significantly relieved the auto-inhibition of Tim *in vitro*, but failed to activate the transforming potential of Tim. It was reasoned that in the cellular environment secondary intermolecular interactions might serve to stabilize the auto-inhibited state. These secondary stabilizing interactions would be lacking in the *in vitro* exchange assays using purified components such that even modest perturbation to the auto-inhibition of Tim (*e.g.* Y22A) would appear relatively enhanced.

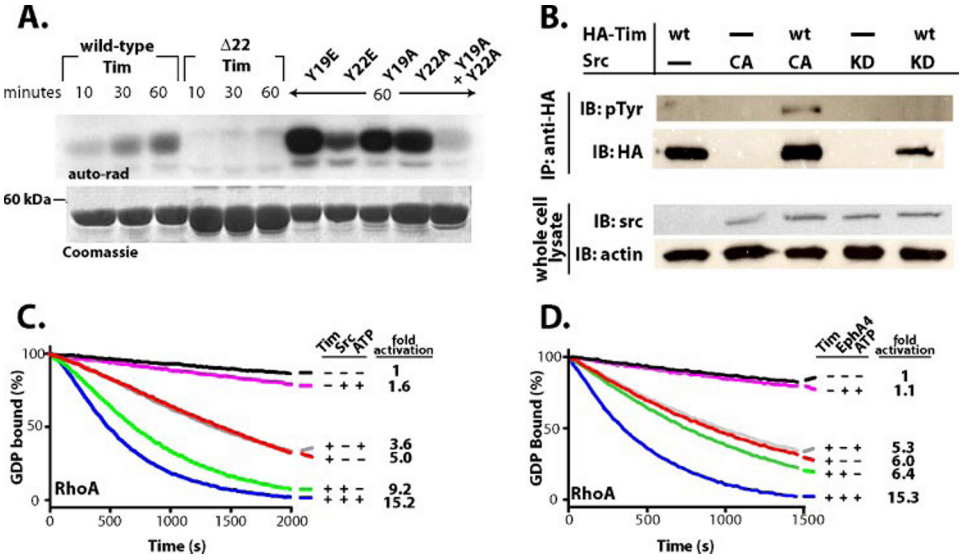

FIGURE 5. **Src phosphorylates Tim and activates its exchange activity.** *A*, Src specifically phosphorylates two tyrosines (19 and 22) within the auto-inhibitory helix of Tim. Purified forms of Tim (*lower panel*) were incubated with recombinant Src and radioactive ATP for various times prior to SDS-PAGE and auto-radiography was used to assess levels of phosphorylation (*upper panel*). Deletion of the entire inhibitory region (Δ22), or tandem substitution of Tyr-19 and Tyr-22 abrogates phosphorylation. *B*, Src phosphorylates Tim *in vivo*. SYF fibroblasts were transiently cotransfected with HA-Tim and constitutively active (*CA*) or kinase dead (*KD*) Src constructs. HA-Tim was immunoprecipitated from cell lysates, and immunoblotted (*IB*) to determine the extent of phosphorylated Tim. The experiment was performed three times and a representative example is shown. Phosphorylation of Tim by Src (*C*) or EphA4 (*D*) promotes the capacity of Tim to catalyze nucleotide exchange on RhoA. Full-length Tim was incubated with combinations of kinase and ATP as indicated for 30 min prior to addition of the mixtures to exchange reactions. -Fold activation is relative to the spontaneous loading of nucleotide onto RhoA (*black trace*) and represents the average of two independent runs for each condition. *wt*, wild type.

To explore this possibility, Tyr-22 was subsequently mutated to Glu (Y22E) with the anticipation that the added negative charge would further perturb auto-inhibitory interactions. The identical substitution was separately created at Tyr-19, and the resulting mutant proteins were analyzed as above. Both potentially phosphomimetic substitutions led to robust *in vitro* activation of RhoA and correspondingly large increases in the transformation potential of Tim. To the best of our knowledge, these data represent the first report of a full-length Dbl-family protein that is activated by single substitutions to the same extent as activation by N-terminal truncation.

To determine whether residues 15–22 of Tim are sufficient for its auto-inhibition, we created a peptide comprising this region and performed an *in vitro* guanine nucleotide exchange assay in which this peptide (*WT*, Fig. 4*A*) was added to Tim (Δ22) in *trans*. The exchange activity of Tim (Δ22) alone was greatly enhanced with respect to full-length Tim, as was also shown in Fig. 1*A*. However, the exchange activity of Tim (Δ22) in the presence of the wild-type peptide was reduced to that of full-length, auto-inhibited Tim. To determine whether the observed inhibition was specific for this peptide, we also created a peptide in which the tyrosine residue corresponding to Tyr-19 in full-length Tim was converted to glutamic acid (*MT*, Fig. 4*A*). Substitution of Tyr-19 with glutamic acid in the context of full-length Tim led to Tim activation in both the *in vitro* exchange assay and the cellular transformation assay (Fig. 3). We therefore expected that a peptide incorporating this substitution would have no effect on the exchange potential of Tim (Δ22). This hypothesis was borne out experimentally, because the exchange potential of Tim (Δ22) in the presence of the mutant peptide was identical to that of Tim (Δ22) alone. Importantly, neither peptide had an effect on the intrinsic rate of exchange on RhoA. These data strongly suggest that residues 15–22 are both necessary and sufficient for Tim auto-inhibition.

To confirm that the N-terminal region is necessary for Tim inhibition in the context of an intact cell, we performed affinity purifications of active Tim using a GST-tagged version of nucleotide-free RhoA (RhoA G17A, Fig. 4*B*). Because Dbl-family proteins bind preferentially to nucleotide-free Rho family GTPases, this construct is expected to affinity purify any active, RhoA-specific GEF present in a cell lysate. Wild-type, HA-tagged Tim, when expressed in serum-starved HEK 293T cells, did not appreciably interact with RhoA G17A. In contrast, both truncated Tim (Δ22) and full-length Tim possessing the double substitution, Y19E + Y22E, were robustly affinity purified by the RhoA G17A matrix, suggesting that the immediate N-terminal region of Tim, and tyrosines 19 and 22 in particular, lead to Tim auto-inhibition by preventing its interaction with RhoA.

Affinity purifications of active RhoA (Fig. 4*C*) confirmed the direct correlation between the capacity of Tim to activate RhoA *in vitro* and the transforming potential of Tim. For example, whereas wild-type Tim did not significantly activate RhoA relative to empty vector upon transfection into HEK 293T cells, both truncated Tim (Δ22) and full-length Tim possessing the double substitution, Y19E + Y22E, dramatically stimulated the loading of GTP onto RhoA. These data strongly suggest that the increased transformation potential of mutant forms of Tim are directly caused by their increased *in vivo* exchange activities.

Regulation of Tim by Tyrosine Phosphorylation—Based upon primary and secondary amino acid sequence analyses, the auto-inhibitory region within Tim is strongly predicted to be helical (residues 16–26; (20)) and tyrosines 19 and 22 within this region are predicted to be excellent substrates for phosphorylation by Src-family non-receptor tyrosine kinases (21). Because the activation of many Dbl-family GEFs is associated with phosphorylation (22), the potential regulation of Tim by phosphorylation was tested both *in vitro* and *in vivo* (Fig. 4). First, it was confirmed that indeed, full-length, purified Tim was an excellent substrate for purified Src, with kinetics and extent of phosphorylation resembling control reactions with a standard, control peptide (Fig. 5*A* and data not shown). Furthermore, phosphorylation was confined to the N-terminal region of Tim, because Src was incapable of phosphorylating Tim (Δ22). Residues 19 and 22 are the only tyrosines encompassed within this

deletion, and both residues are phosphorylated by Src because substitution at both sites (Y19A + Y22A) is required to prevent the phosphorylation of full-length Tim. Intriguingly, single substitution at either Tyr-19 or Tyr-22 enhances phosphorylation at the other tyrosine, indicating that the two sites might be functionally linked. One simple interpretation for these data posits that substitution at either tyrosine significantly disrupts intramolecular interactions associated with auto-inhibition such that the remaining tyrosine is more accessible for phosphorylation by Src.

A logical extension of this scenario is that phosphorylation at tyrosines 19 and 22 might be physiologically relevant for relieving the auto-inhibition of Tim *in vivo*. Consequently, it was shown that constitutively active but not kinase dead (KD) Src was capable of phosphorylating Tim *in vivo* upon co-expression in SYF fibroblasts designed to lack endogenous Src-family kinases (Fig. 5*B*). In the same vein, Src robustly activated Tim *in vitro* using purified components (Fig. 5*C*). In this setting, maximal activation required ATP consistent with the idea that phosphorylation of Tim by Src relieves auto-inhibition of Tim to promote activation of RhoA. Taken together, these data strongly suggest that the *in vivo* phosphorylation of Tim within its auto-inhibitory region by Src might be a physiologically relevant means of activating the exchange potential of Tim and linking as yet unidentified upstream cellular events with the activation of RhoA.

Src without ATP also activated Tim (Fig. 5*C*), suggesting that the binding of Src to Tim partially disrupted the auto-inhibition of Tim. However, the possibility exists that Src remained bound to ATP during purification of the kinase domain, and that additional ATP is not required for this kinase domain to phosphorylate Tim. To test this hypothesis, we incubated Tim with increasing amounts of the purified Src kinase domain and performed a phosphotyrosine blot (Fig. 6*A*). Auto-phosphorylation of the kinase domain, and phosphorylation of Tim, only occurred when ATP was included in the reaction, suggesting that the purified Src kinase domain is not bound to ATP. To confirm that Src binding to Tim, in the absence of phosphorylation, activates Tim, we also performed an exchange assay in which Tim was incubated with a kinase inactive (K297A) version of Src (Fig. 6*B*). Kinase inactive Src was also able to activate Tim, indicating that formation of a complex between Src and Tim, decoupled from phosphorylation, is sufficient to partially activate the exchange capacity of Tim. We have been unable to isolate a complex of Tim and Src by co-immunoprecipitation experiments from cells over-expressing both of the proteins (data not shown), suggesting that their interaction is transient *in vivo* where endogenous concentrations of ATP favor completion of the phosphorylation reaction.

The Tim homologs, ephexin and Vsm-RhoGEF, interact with and are tyrosine phosphorylated downstream of the EphA4 receptor tyrosine kinase (23, 24). To test the hypothesis that Tim is directly phosphorylated by EphA4, we performed *in vitro* kinase assays with the recombinant kinase domain of EphA4. Tim was robustly phosphorylated by the kinase domain of EphA4 (data not shown), indicating that Tim is phosphorylated by EphA4 directly. Additionally, EphA4 activated Tim *in vitro* (Fig. 5*D*). In this case, the kinase in the absence of ATP did not activate Tim, suggesting

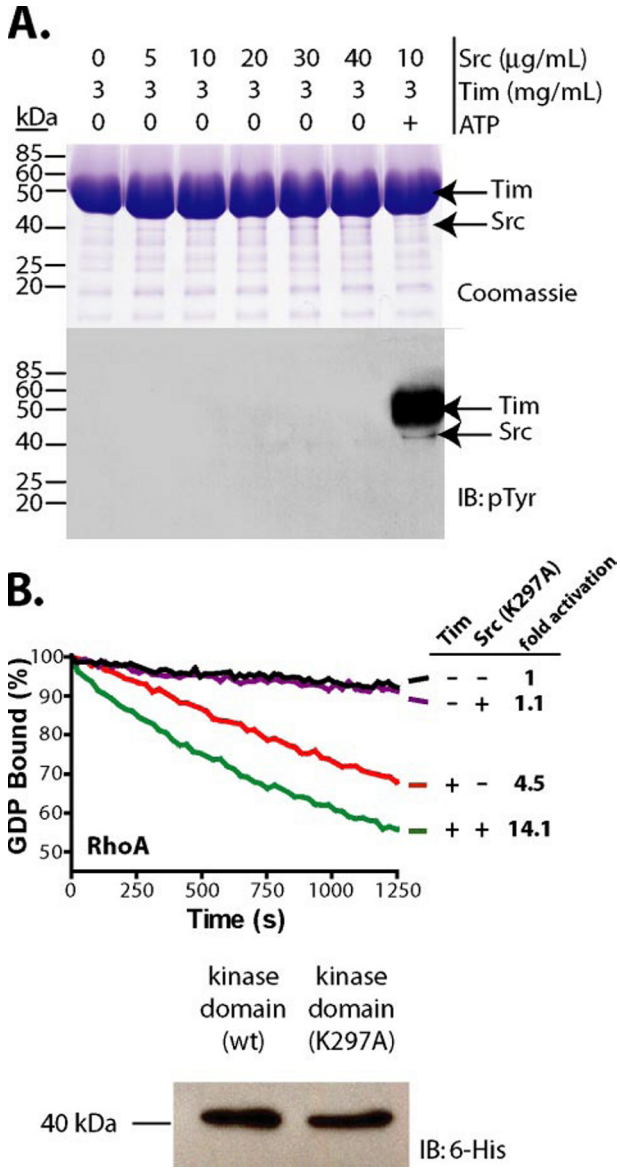

FIGURE 6. **The Src kinase domain activates Tim in the absence of phosphorylation.** *A*, ATP is required for the phosphorylation of Tim by recombinant Src produced in baculovirus-infected HighFive cells. Various combinations of Tim and Src were incubated for 30 min at 37 °C prior to SDS-PAGE and immunoblot (*IB*) analysis. *B*, kinase-inactive Src activates Tim. Full-length Tim was incubated with combinations of kinase-inactive Src as indicated for 30 min prior to addition of the mixtures to exchange reactions. -Fold activation is relative to the spontaneous loading of nucleotide onto RhoA (*black trace*) and represents the average of two independent runs for each condition. Equal amounts of the purified Src proteins are shown in the *lower panel* following immunoblot analysis.

that the interaction between EphA4 and Tim is transient compared with the interaction between Tim and Src. These data suggest that binding of ligand to the EphA4 receptor may lead to the phosphorylation and activation of Tim.

Disrupting Auto-inhibition by Mutating the DH Domain—The above experiments have shown that Tim is auto-inhibited by a small, conserved region with high helical propensity and that this auto-inhibition can be relieved by truncation, mutation, or phosphorylation of the auto-inhibitory region. This situation is reminiscent of regulation of the Vav isozymes whereby a short helix immediately preceding the DH domain lies down

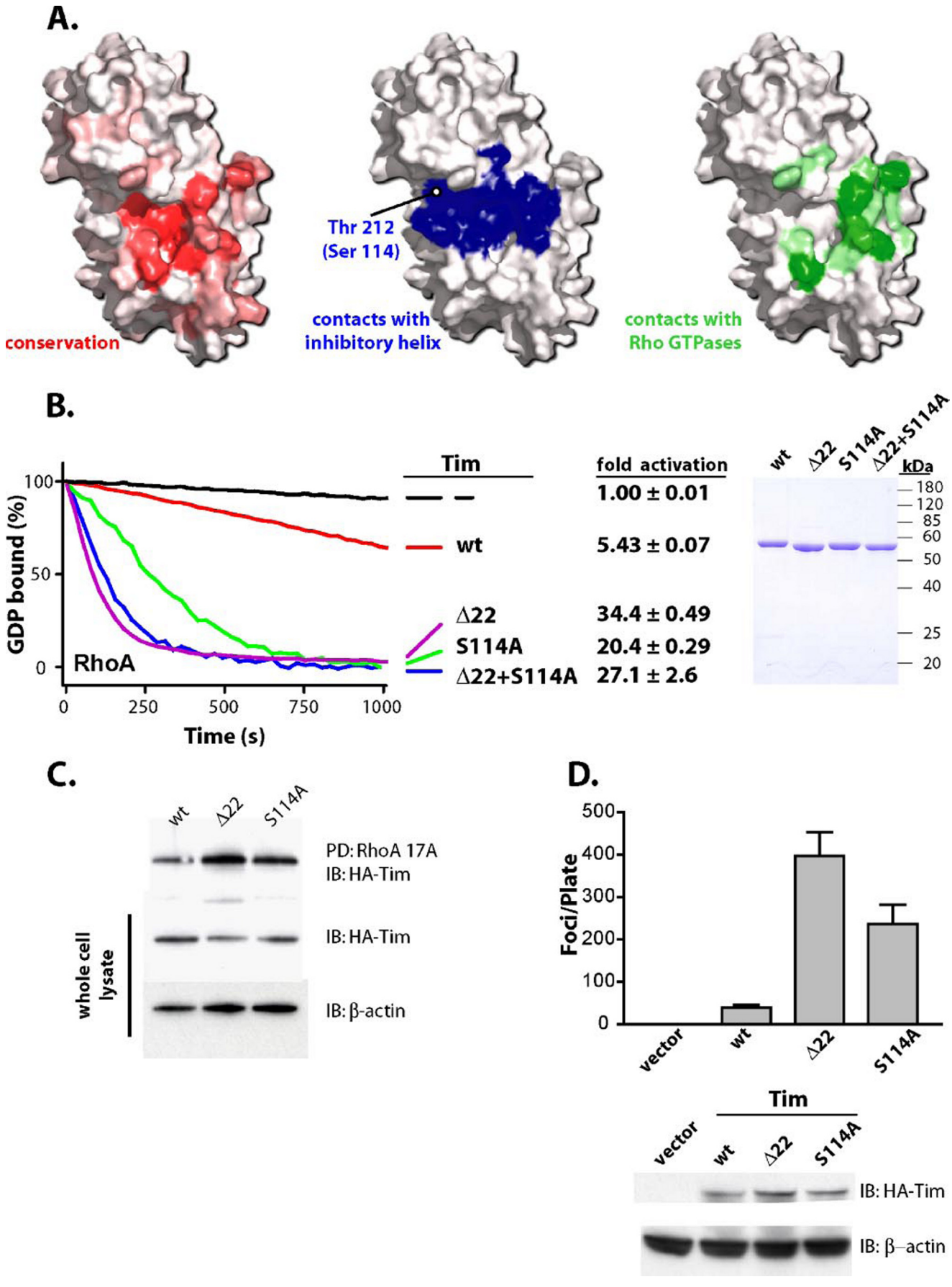
A.
conservation
Thr 212
(Ser 114)
contacts with
inhibitory helix
contacts with
Rho GTPases
B.
GDP bound (%)
100
50
0
RhoA
0
250
500
750
1000
Time (s)
Tim
fold activation
wt
1.00 ± 0.01
wt
5.43 ± 0.07
Δ22
34.4 ± 0.49
S114A
20.4 ± 0.29
Δ22+S114A
27.1 ± 2.6
wt
Δ22
S114A
Δ22+S114A
kDa
180
120
85
60
50
40
25
20
C.
wt
Δ22
S114A
PD: RhoA 17A
IB: HA-Tim
IB: HA-Tim
whole cell
lysate
IB: β-actin
D.
Foci/Plate
500
400
300
200
100
0
vector
wt
Δ22
S114A
Tim
vector
wt
Δ22
S114A
IB: HA-Tim
IB: β–actin

on the most conserved surface of the DH domain to prevent Rho GTPases from engaging this same surface for effective nucleotide exchange (25). Phosphorylation of the inhibitory helix in the Vav isozymes by Src and related non-receptor tyrosine kinases stimulates exchange *in vitro* and *in vivo* (26–30) and is required for some physiological functions of Vav (31). If a similar mechanism is operative for Tim, then it might be possible to mutate specific residues within the DH domain to disrupt interactions with the auto-inhibitory helix without affecting GTPase binding, and in this way constitutively activate Tim. Such residues within the DH domain would be expected to be conserved, equivalent to sites that contact the auto-inhibitory helix of Vav1, and yet not critical for the interaction of the DH domain with GTPases. Appropriate analyses of the available sequence and structure data (Fig. 7*A*) identified several sites that fit these criteria, and Tim was mutated with individual substitutions (Y111L and S114A) to test this hypothesis. Tim (Y111L) was destabilized, insoluble and inactive *in vitro* (data not shown). In contrast, Tim (S114A) is stable, soluble, and able to activate RhoA *in vitro* (Fig. 7*B*) ~4-fold more efficiently than wild-type Tim. Importantly, under identical conditions, S114A is relatively silent within the context of Tim lacking the auto-inhibitory helix (Δ22), indicating that the intrinsic exchange mechanism of Tim is unaffected by S114A. The ability of this mutant (Δ22 + S114A) to catalyze exchange, however, is inhibited by addition of 100 μM of the peptide corresponding to the N-terminal putative helical motif (residues 15–25) of Tim used in Fig. 4*A* (data not shown). This result indicates that the S114A substitution does not completely abolish the interaction between the N-terminal auto-inhibitory motif of Tim and the DH domain pocket and is consistent with the partial relief of inhibition of exchange caused by the S114A substitution within the context of full-length Tim (Fig. 7*A*).

Consistent with the *in vitro* exchange data, Tim (S114A) behaved similarly to truncated Tim (Δ22) in its ability to interact with nucleotide-free RhoA (Fig. 7*C*) and its ability to induce formation of foci (Fig. 7*D*). Consequently, it is possible to decouple the auto-inhibitory and exchange functions of Tim through mutation of its DH domain.

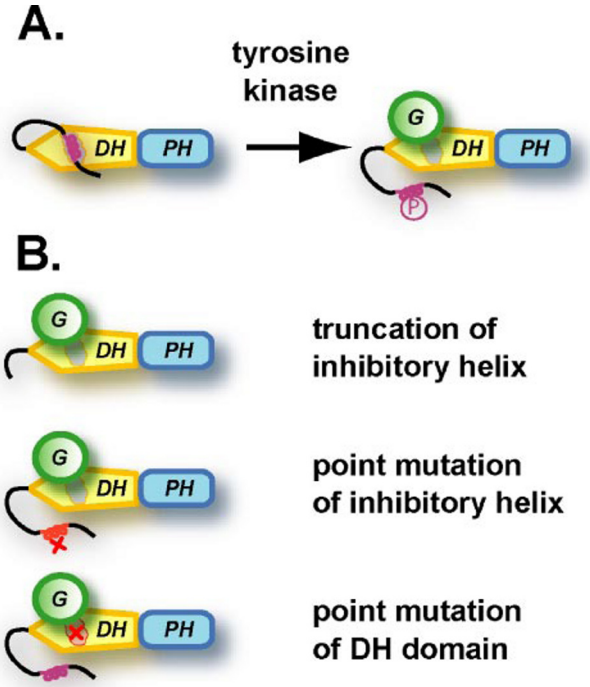

FIGURE 8. **Model of Tim auto-inhibition.** *A*, regulation of Tim exchange activity by sequences N-terminal to the DH domain. The auto-inhibitory helix packs against the conserved pocket of the DH domain, preventing the binding and consequent activation of the cognate Rho GTPase. Tyrosine phosphorylation leads to the removal of the auto-inhibitory helix from the DH domain. Tim can now bind Rho to catalyze the exchange of guanine nucleotide. *B*, mechanisms of constitutive activation of Tim proteins. The auto-inhibitory helix is truncated, or otherwise mutated such that it can no longer bind to the DH domain. Alternatively, residues within the conserved binding patch of the DH domain are mutated such that it is no longer able to bind the auto-inhibitory helix, leading to a constitutively active GEF. In each of these scenarios, the end result is loss of auto-inhibition leading to constitutive activation of Tim.

DISCUSSION

Fig. 8 presents a model for the relief of auto-inhibition of Tim. In this model, an auto-inhibitory helix packs against the conserved pocket of the DH domain in the basal, inactive state to prevent Rho GTPases from accessing the surface of the DH domain necessary for guanine nucleotide exchange. Activation of Src leads to phosphorylation of the auto-inhibitory helix, which disrupts the interactions between the auto-inhibitory helix and the DH domain, thereby freeing the DH domain to interact with cognate GTPases and activate them by nucleotide exchange. If the auto-inhibitory helix is truncated, or otherwise mutated such that it can no longer bind to the DH domain, Tim will be constitutively activated. Likewise, if residues within the conserved binding patch of the DH domain are mutated such

FIGURE 7. **Mutations within the DH domain designed to disrupt the interaction with the auto-inhibitory helix lead to auto-activation.** *A*, surface representations of the Vav1 DH domain (Protein Data Bank accession 1F5X, murine Vav1 residues 198–372) that illustrate: *left*, the positions of highly conserved residues among DH domains from 70 human Dbl-family sequences as determined by ClustalX (*bright red* is most conserved); *center*, the sites of contact (≤5 Å; *blue*) between the Vav1 DH domain and the Vav1 auto-inhibitory helix (residues 170–179); and *right*, the sites and degree of conservation of interactions observed within the structures of Tiam1·Rac1, Intersectin·Cdc42, Dbs·RhoA, and Larg·RhoA that occur between Rho GTPases and DH domains (≤3.5 Å between residues, *bright green* is fully conserved) mapped onto the surface of the DH domain of Vav1. Surface representations were produced using the programs ProtSkin (49) and PyMOL (50) and reveal a region of high sequence conservation in a pocket that contacts the auto-inhibitory helix but does not contact Rho GTPases. Thr-212 of Vav1 is indicated and the equivalent residue (Ser-114) in Tim has been mutated to disrupt auto-inhibition as shown below. *B*, relative to the spontaneous loading of guanine nucleotide onto RhoA (−, *black trace*) auto-inhibition of full-length Tim (wt, *red trace*) is relieved by mutation within its DH domain (S114A, *green trace*), whereas the exchange activity of truncated, constitutively active Tim (Δ22, *magenta trace*) is relatively unaffected by the equivalent mutation (Δ22 + S114A, *blue trace*). The traces corresponding to spontaneous loading, full-length Tim, and Tim (Δ22) are reproduced from Fig. 2 for reference. Proteins used in the exchange assays are shown at *right*. *C*, the S114A mutation increases the ability of Tim transiently expressed in quiescent HEK 293T cells to associate with nucleotide-free RhoA. The activity level of Tim constructs was assessed as described in the legend to Fig. 4. Levels of active Tim were determined by immunoblotting the pulldown samples. Immunoblots (*IB*) of the total cell lysate (2.5% input shown) show approximately equal expression of the Tim constructs. *D*, mutation in the DH domain (S114A) increases the ability of Tim to induce foci when expressed in NIH 3T3 cells. Data represent the averages of three independent experiments carried out in duplicate. The *lower panel* shows approximately equal expression of the Tim constructs.

that it is no longer able to bind the auto-inhibitory helix, Tim will be constitutively activated.

Tim clusters with five other human Dbl-family proteins: neuroblastoma, Sgef, Wgef, Ngef, and Vsm-RhoGEF, based on high sequence identity among DH domains and overall domain architecture that includes an SH3 domain C-terminal to the canonical DH/PH module. Whereas not readily evident using standard sequence alignment algorithms such as PSI-BLAST, all members of this subgroup possess a putative auto-inhibitory region N-terminal to the DH domain with high sequence identity to the short auto-inhibitory region mapped in Tim (data not shown). Consequently, it is likely that other members of this subgroup are regulated in a manner similar to Tim. In fact, the mouse homolog of Ngef, ephexin, is tyrosine phosphorylated in an N-terminal motif with significant sequence identity to the auto-inhibitory helix within the Tim subgroup of Dbl proteins. However, phosphorylation of ephexin alters its exchange profile. Specifically, unphosphorylated ephexin activates RhoA, Rac1, and Cdc42; but when tyrosine phosphorylated, ephexin exclusively activates RhoA (32). The mechanism by which this specificity switch occurs is currently unknown and not encompassed within the model presented here for the activation of Tim.

The mechanism of auto-inhibition of Tim presented above is reminiscent of the mechanism of auto-inhibition of the Vav isozymes. In fact, the auto-inhibitory helix of Tim shows high sequence homology to the auto-inhibitory helix of Vav1 (data not shown). The structure of an extended fragment of the DH domain of Vav1 highlights the steric occlusion of the DH domain through interaction with an N-terminal helix to prevent GTPase binding and guanine nucleotide exchange (25). This inhibition is relieved upon phosphorylation of Tyr-174 within the inhibitory helix, which disrupts the interaction of the inhibitory helix with the DH domain and allows Rho GTPases to access the catalytic surface of the DH domain for effective guanine nucleotide exchange. Whereas this regulatory mechanism is operative *in vivo* for the three Vav isozymes, complete regulation of Vav isozymes is more complex. For example, Vav1 is additionally phosphorylated at Tyr-142 and Tyr-160 within a highly acidic region, and substitution of all three tyrosines to phenylalanine greatly enhances the transformation potential of full-length Vav1 relative to any single substitution. However, a mutant of Vav1 truncated to remove its N-terminal calponin homology domain, but not the phosphorylated tyrosines, is also transforming, suggesting that the calponin homology domain stabilizes interactions of the auto-inhibitory helix with the DH domain within the context of full-length Vav1 (7). In addition, the calponin homology domain contributes to the auto-inhibition of Vav proteins by interacting with a cysteine-rich domain C-terminal to the DH/PH cassette (33, 34). Furthermore, Vav proteins may also be regulated allosterically through the binding of phospholipids to the PH domain, although this concept remains controversial (35, 36). Thus, the regulated activation of the Vav isozymes is more complex than what we have shown above for Tim because the activation of Vav isozymes cannot be attributed solely to the phosphorylation of tyrosine residues N-terminal to the DH domain.

The human genome encodes 58 receptor tyrosine kinases, and more than half of the receptor tyrosine kinases are known to activate at least one of the Rho family members. At least 16 of the 69 human Dbl-family proteins are known to interact with and/or be phosphorylated by receptor tyrosine kinases, thus serving as a link between ligation of receptor tyrosine kinases and Rho activation (22). For instance, FRG, a Dbl-family protein specific for Cdc42, is activated upon phosphorylation by Src downstream of signals arising from both the endothelin A receptor (37) and nectins (38). Similarly, the exchange activity of Dbs for Cdc42 is enhanced upon the phosphorylation of Dbs by Src downstream of the α1B adrenergic receptor (39). Activated TrkB directly binds to and activates Tiam1 (40), which is also known to be phosphorylated and activated by Src (41). In each case mentioned above, the mechanisms by which phosphorylation increases exchange activity have yet to be determined. Clearly, one fruitful avenue of research will be to assess mechanistically how these phosphorylations enhance exchange; one likely mechanism is that phosphorylation perturbs auto-inhibition as described here.

The Rho GTPases have long been thought to play a role in tumorigenesis. However, in contrast to Ras GTPases, animal studies and studies of human tumors have yet to further our understanding of the role of Rho GTPases in promoting tumorigenesis. In fact, constitutively active, GTPase-deficient mutants of Rho GTPases have yet to be found in human tumors. However, several Rho GTPases, including RhoA, RhoC, and Rac1, are over-expressed in human tumors, leading to the hypothesis that Rho GTPases, unlike Ras GTPases, must undergo cycling of GTP loading to be oncogenic (3, 42). Consistent with this idea, Dbl-family Rho GEFs are more potent oncogenes than their substrate GTPases. Although many Dbl-family proteins, including Tim, were identified as proto-oncogenes in expression library screens using DNA or RNA derived from human cancer cells, these activation events have proven to be experimental artifacts. Of the 69 human Dbl-family proteins, only Tiam1 has been shown to be mutated in human tumors (4), although Vav1 is ectopically expressed in some primary pancreatic adenocarcinomas (43) and neuroblastomas (44). The mutations characterized in this study, both in the auto-inhibitory helix and DH domain, represent potential mechanisms by which Tim and other Dbl-family proteins might be activated in human tumors. Identification of such mutations in human tumors would further define the role of Rho GTPases in tumorigenesis.

If versions of Tim mutated in either the auto-inhibitory helix or in the region of the DH domain thought to interact with the auto-inhibitory helix should be isolated from human tumors, then Tim would represent an attractive target for rational drug design. The peptide inhibitor shown in Fig. 3*A* could serve as the basis for design of peptidomimetic inhibitors of aberrant Tim activation of Rho. Several inhibitors of small GTPase activation have been previously identified. TRIPα was isolated as a random peptide aptamer that selectively binds to the second DHPH cassette of the RhoGEF Trio and inhibits the exchange activity of Trio *in vitro* and in PC12 cells through an unknown mechanism (45). Additionally, the small molecule NCS23766 was identified in structure-based virtual screen for compounds that might fit into a pocket on the surface of Rac1. Residues in this pocket contact Tiam1 during the exchange reaction. This compound selectively inhibits Rac1 binding to Rac1-specific

GEFs *in vitro* and prevents platelet-derived growth factor-induced Rac activation in cells (46, 47). Finally, brefeldin A inhibits the activation of the small GTPase Arf1 by its exchange factors by binding to and stabilizing a complex of Arf1-GDP and the catalytic Sec7 domain (48). The Tim peptide, then, is a unique GEF inhibitor in that its mechanism of action is identical to that of the auto-inhibitory helix of the wild-type protein.

In summary, we have shown that the Dbl-family protein, Tim, is a RhoA-, RhoB-, and RhoC-specific GEF that is auto-inhibited by a putative helix N-terminal to the DH domain, which directly binds the DH domain to sterically exclude Rho GTPases and prevent their activation. This auto-inhibition is relieved by truncation, mutation, or phosphorylation of the auto-inhibitory helix, or by mutation of the conserved surface of the DH domain to disrupt interactions with the auto-inhibitory helix. Because inhibition of Tim can be restored by addition of the auto-inhibitory helix in *trans*, the auto-inhibitory helix is necessary and sufficient for maintenance of a basal state of Tim activation.

Acknowledgments—We thank Cynthia Holley, Dr. Mark Jezyk, and Dr. Carol Winkelman for critical reading of the manuscript and Drs. David Siderovski and Keith Burridge for helpful discussions and reagents.

REFERENCES

1. Wennerberg, K., and Der, C. J. (2004) *J. Cell Sci.* **117,** 1301–1312
2. Etienne-Manneville, S., and Hall, A. (2002) *Nature* **420,** 629–635
3. Sahai, E., and Marshall, C. J. (2002) *Nat. Rev. Cancer* **2,** 133–142
4. Rossman, K. L., Der, C. J., and Sondek, J. (2005) *Nat. Rev. Mol. Cell. Biol.* **6,** 167–180
5. Yoshizuka, N., Moriuchi, R., Mori, T., Yamada, K., Hasegawa, S., Maeda, T., Shimada, T., Yamada, Y., Kamihira, S., Tomonaga, M., and Katamine, S. (2004) *J. Biol. Chem.* **279,** 43998–44004
6. Vanni, C., Mancini, P., Gao, Y., Ottaviano, C., Guo, F., Salani, B., Torrisi, M. R., Zheng, Y., and Eva, A. (2002) *J. Biol. Chem.* **277,** 19745–19753
7. Lopez-Lago, M., Lee, H., Cruz, C., Movilla, N., and Bustelo, X. R. (2000) *Mol. Cell. Biol.* **20,** 1678–1691
8. Zenke, F. T., Krendel, M., DerMardirossian, C., King, C. C., Bohl, B. P., and Bokoch, G. M. (2004) *J. Biol. Chem.* **279,** 18392–18400
9. Schmidt, A., and Hall, A. (2002) *Genes Dev.* **16,** 1587–1609
10. Chan, A. M., McGovern, E. S., Catalano, G., Fleming, T. P., and Miki, T. (1994) *Oncogene* **9,** 1057–1063
11. Xie, X., Chang, S. W., Tatsumoto, T., Chan, A. M., and Miki, T. (2005) *Cell. Signal.* **17,** 461–471
12. Takai, S., Chan, A. M., Yamada, K., and Miki, T. (1995) *Cancer Genet. Cytogenet.* **83,** 87–89
13. Debily, M. A., Camarca, A., Ciullo, M., Mayer, C., El Marhomy, S., Ba, I., Jalil, A., Anzisi, A., Guardiola, J., and Piatier-Tonneau, D. (2004) *Hum. Mol. Genet.* **13,** 323–334
14. Worthylake, D. K., Rossman, K. L., and Sondek, J. (2000) *Nature* **408,** 682–688
15. Rossman, K. L., Worthylake, D. K., Snyder, J. T., Siderovski, D. P., Campbell, S. L., and Sondek, J. (2002) *EMBO J.* **21,** 1315–1326
16. Snyder, J. T., Worthylake, D. K., Rossman, K. L., Betts, L., Pruitt, W. M., Siderovski, D. P., Der, C. J., and Sondek, J. (2002) *Nat. Struct. Biol.* **9,** 468–475
17. Rojas, R. J., Kimple, R. J., Rossman, K. L., Siderovski, D. P., and Sondek, J. (2003) *Comb. Chem. High Throughput Screen* **6,** 409–418
18. Solski, P. A., Wilder, R. S., Rossman, K. L., Sondek, J., Cox, A. D., Campbell, S. L., and Der, C. J. (2004) *J. Biol. Chem.* **279,** 25226–25233
19. Arthur, W. T., Ellerbroek, S. M., Der, C. J., Burridge, K., and Wennerberg, K. (2002) *J. Biol. Chem.* **277,** 42964–42972
20. Rost, B. (1996) *Methods Enzymol.* **266,** 525–539
21. Blom, N., Gammeltoft, S., and Brunak, S. (1999) *J. Mol. Biol.* **294,** 1351–1362
22. Schiller, M. R. (2006) *Cell. Signal.* **18,** 1834–1843
23. Ogita, H., Kunimoto, S., Kamioka, Y., Sawa, H., Masuda, M., and Mochizuki, N. (2003) *Circ. Res.* **93,** 23–31
24. Shamah, S. M., Lin, M. Z., Goldberg, J. L., Estrach, S., Sahin, M., Hu, L., Bazalakova, M., Neve, R. L., Corfas, G., Debant, A., and Greenberg, M. E. (2001) *Cell* **105,** 233–244
25. Aghazadeh, B., Lowry, W. E., Huang, X. Y., and Rosen, M. K. (2000) *Cell* **102,** 625–633
26. Miranti, C. K., Leng, L., Maschberger, P., Brugge, J. S., and Shattil, S. J. (1998) *Curr. Biol.* **8,** 1289–1299
27. Salojin, K. V., Zhang, J., Meagher, C., and Delovitch, T. L. (2000) *J. Biol. Chem.* **275,** 5966–5975
28. Teramoto, H., Salem, P., Robbins, K. C., Bustelo, X. R., and Gutkind, J. S. (1997) *J. Biol. Chem.* **272,** 10751–10755
29. Han, J., Das, B., Wei, W., Van Aelst, L., Mosteller, R. D., Khosravi-Far, R., Westwick, J. K., Der, C. J., and Broek, D. (1997) *Mol. Cell. Biol.* **17,** 1346–1353
30. Crespo, P., Schuebel, K. E., Ostrom, A. A., Gutkind, J. S., and Bustelo, X. R. (1997) *Nature* **385,** 169–172
31. Fischer, K. D., Zmuldzinas, A., Gardner, S., Barbacid, M., Bernstein, A., and Guidos, C. (1995) *Nature* **374,** 474–477
32. Sahin, M., Greer, P. L., Lin, M. Z., Poucher, H., Eberhart, J., Schmidt, S., Wright, T. M., Shamah, S. M., O'Connell, S., Cowan, C. W., Hu, L., Goldberg, J. L., Debant, A., Corfas, G., Krull, C. E., and Greenberg, M. E. (2005) *Neuron* **46,** 191–204
33. Zugaza, J. L., Lopez-Lago, M. A., Caloca, M. J., Dosil, M., Movilla, N., and Bustelo, X. R. (2002) *J. Biol. Chem.* **277,** 45377–45392
34. Llorca, O., Arias-Palomo, E., Zugaza, J. L., and Bustelo, X. R. (2005) *EMBO J.* **24,** 1330–1340
35. Han, J., Luby-Phelps, K., Das, B., Shu, X., Xia, Y., Mosteller, R. D., Krishna, U. M., Falck, J. R., White, M. A., and Broek, D. (1998) *Science* **279,** 558–560
36. Das, B., Shu, X., Day, G. J., Han, J., Krishna, U. M., Falck, J. R., and Broek, D. (2000) *J. Biol. Chem.* **275,** 15074–15081
37. Miyamoto, Y., Yamauchi, J., and Itoh, H. (2003) *J. Biol. Chem.* **278,** 29890–29900
38. Fukuhara, T., Shimizu, K., Kawakatsu, T., Fukuyama, T., Minami, Y., Honda, T., Hoshino, T., Yamada, T., Ogita, H., Okada, M., and Takai, Y. (2004) *J. Cell Biol.* **166,** 393–405
39. Yamauchi, J., Hirasawa, A., Miyamoto, Y., Kokubu, H., Nishii, H., Okamoto, M., Sugawara, Y., Tsujimoto, G., and Itoh, H. (2002) *Biochem. Biophys. Res. Commun.* **296,** 85–92
40. Miyamoto, Y., Yamauchi, J., Tanoue, A., Wu, C., and Mobley, W. C. (2006) *Proc. Natl. Acad. Sci. U. S. A.* **103,** 10444–10449
41. Servitja, J. M., Marinissen, M. J., Sodhi, A., Bustelo, X. R., and Gutkind, J. S. (2003) *J. Biol. Chem.* **278,** 34339–34346
42. Boettner, B., and Van Aelst, L. (2002) *Gene* (*Amst.*) **286,** 155–174
43. Fernandez-Zapico, M. E., Gonzalez-Paz, N. C., Weiss, E., Savoy, D. N., Molina, J. R., Fonseca, R., Smyrk, T. C., Chari, S. T., Urrutia, R., and Billadeau, D. D. (2005) *Cancer Cell* **7,** 39–49
44. Hornstein, I., Pikarsky, E., Groysman, M., Amir, G., Peylan-Ramu, N., and Katzav, S. (2003) *J. Pathol.* **199,** 526–533
45. Schmidt, S., Diriong, S., Mery, J., Fabbrizio, E., and Debant, A. (2002) *FEBS Lett.* **523,** 35–42
46. Akbar, H., Cancelas, J., Williams, D. A., Zheng, J., and Zheng, Y. (2006) *Methods Enzymol.* **406,** 554–565
47. Gao, Y., Dickerson, J. B., Guo, F., Zheng, J., and Zheng, Y. (2004) *Proc. Natl. Acad. Sci. U. S. A.* **101,** 7618–7623
48. Zeeh, J. C., Zeghouf, M., Grauffel, C., Guibert, B., Martin, E., Dejaegere, A., and Cherfils, J. (2006) *J. Biol. Chem.* **281,** 11805–11814
49. Deprez, C., Lloubes, R., Gavioli, M., Marion, D., Guerlesquin, F., and Blanchard, L. (2005) *J. Mol. Biol.* **346,** 1047–1057
50. DeLano, W. L. (2002) *The PyMOL Molecular Graphics System*, DeLano Scientific, San Carlos, CA
51. Snyder, J. T., Singer, A. U., Wing, M. R., Harden, T. K., and Sondek, J. (2003) *J. Biol. Chem.* **278,** 21099–21104